Graphene modification with gold nanoparticles using the gas aggregation technique

L.E.G. Armas [a,*], G.T. Landi [b], M.F.G. Huila [c], A. Champi [d], M. Pojar [a], A.C. Seabra [a], A.D. Santos [b], K. Araki [c], H.E. Toma [c,**]

[a] Escola Politécnica, Laboratório de Sistemas Integráveis da Universidade de São Paulo, CEP 05508-010, São Paulo, SP, Brazil
[b] Insitituto de Física, Laboratorio de Materiais Magnéticos, da Universidade de São Paulo, CP 66318, São Paulo, SP, Brazil
[c] Instituto de Química, Laboratório de Nanotecnologia, da Universidade de São Paulo, CP 26077, São Paulo, SP, Brazil
[d] Centro de Ciências Naturais e Humanas da Universidade Federal do ABC-São Paulo, CEP 09210-170, São Paulo, SP, Brazil

ARTICLE INFO

ABSTRACT

Gold nanoparticles (Au-NPs) were deposited on single layer graphene (SLG) and few layers graphene (FLG) by applying the gas aggregation technique, previously adapted to a 4-gun commercial magnetron sputtering system. The samples were supported on SiO_2 (280 nm)/Si substrates, and the influence of the applied DC power and deposition times on the nanoparticle–graphene system was investigated by Confocal Raman Microscopy. Analysis of the G and 2D bands of the Raman spectra shows that the integrated intensity ratio (I_{2D}/I_G) was higher for SLG than for FLG. For the samples produced using a sputtering power of 30 W, the intensity (peak height) of the G and 2D bands increased with the deposition time, whereas for those produced applying 60 W the peak heights of the G and 2D bands decreased with the deposition time. This behaviour was ascribed to the formation of larger Au-NPs aggregates in the last case. A significant increase of the Full Width Half Maximum (FWHM) of the G band for SLG and FLG was also observed as a function of the DC power and deposition time. Surprisingly, the fine details of the Raman spectra revealed an unintentional doping of SLG and FLG accompanying the increase of size and aggregation of the Au-NPs.

1. Introduction

Graphene was first isolated in 2004 [1] by the micromechanical cleavage of graphite crystals, and since then it became one of the most intensively studied materials owing to its unique physical properties and potential applications [2–4]. The micromechanical procedure has not yet been abandoned, since at the present time, the preparation of monolayer or few layers graphene in large sizes or in defect-free states remains very challenging [5,6].

A convenient tool for the characterization of graphene is Raman spectroscopy, because it is able to identify the number of layers, the electronic structure, the edge structure, the type of doping and also structural defects [7]. The graphene Raman spectra collected at visible excitation wavelengths exhibit very characteristic peaks, which have been extensively studied [8–10]. A peak near 1580 cm^{-1}, also known as the G band, has been assigned to an in-plane asymmetric translational motion of two nearby carbon atoms (E_{2g} mode). This is a degenerated optical phonon mode at the Brillouin zone centre (the Γ point of the reciprocal lattice space), and is induced by a single resonance process. There is another peak around 1300–1400 cm^{-1}, denoted as the D band, which corresponds to an in-plane carbon ring breathing mode (A_{1g} mode). This band is symmetry forbidden

in perfect graphite. The peak position of the D band is dependent upon the excitation wavelength, and has been explained by a double resonance process at the K point of the reciprocal lattice space. This process requires a scattering at defect sites in order to conserve the momentum. For this reason, the D band has been considered a measure of disorder in graphite crystals, and it is dominant at the edge sites of single layer graphene [11]. The double resonance process also induces an additional activation by two phonons appearing around 2600–2800 cm^{-1}. Since this peak frequency is practically double of the frequency of the D band, it is has been denoted 2D. Interestingly, the 2D peak position is sensitive to the excitation wavelength and perturbations on the graphene layer and its band shape can be used to identify the number of graphene layers [7,8,12].

Currently, Raman spectroscopy has also been employed to monitor the doping in graphene [13,14]. It should be noted that the ability to control the n or p doping is a key point for electronic applications. The effect of back-gating and top-gating on the G-peak position and its FWHM has been reported in the literature [13–15]. In addition, the G-peak frequency increases while the FWHM(G) decreases for both electron and hole doping. The stiffening of the G peak is due to the non-adiabatic removal of the Kohn-anomaly at Γ [15]. The FWHM sharpening is due to blockage of the phonon decay into electron hole pairs due to the Pauli exclusion principle, when the electron–hole gap becomes higher than the phonon energy [15,16]. FWHM(G) sharpening saturates when the doping causes a Fermi level shift greater than half of the phonon energy [15]. Doping has been studied in single layer

* Correponding author. Tel.: + 55 11 3091 9706; fax: + 55 11 3091 5665 .
E-mail addresses: legarmas@gmail.com (L.E.G. Armas), henetoma@iq.usp.br (H.E. Toma).

graphene with aromatic molecules [17], in suspended and non suspended graphene (SG and NSG) [18]. It has been found that the intensity ratio between the 2D and G bands is a sensitive indicator, of the level of charged impurities present [18]. It has also been shown that molecules which act as electron-donors or acceptors modify the electronic structure of single-walled carbon nanotubes (SWNTs), giving rise to significant changes in the electronic and Raman spectra as well as in their electrical properties [19,20].

Recently, graphene has been successfully modified with gold nanoparticles (Au-NPs) using conventional synthetic strategies [21,22], by the in situ reduction of $HAuCl_4$ or the direct interaction with previously formed Au-NPs.

To the best of our knowledge, graphene modification with gold nanoparticles using the gas aggregation technique has never been reported before. In addition to its rather simple nature, this technique allows the controlled deposition of gold clusters without the interference of any chemical coating, as in the case of most typical chemical procedures. There is also especial interest in the generation of graphene containing gold nanoparticles for catalysis [23]. The gas aggregation technique is based on the vapour phase condensation of sputtered atoms. The nanoparticles produced were deposited directly over graphene in a 4-gun commercial magnetron sputtering system [24]. This methodology was employed here for exploring a new route of modification of graphene with gold nanoparticles using two different DC sputtering powers and deposition times. The Raman signals were recorded for SLG and FLG before and after depositing the Au-NPs, and the integrated intensity ratio of the 2D and G bands (I_{2D}/I_G) as well as their FWHM was investigated as a function of time and G band frequency shift, for the two DC power depositions, after deconvoluting using Lorentzian functions. The measurements were performed for each region of SLG and FLG.

2. Samples and experimental details

A set of four samples were prepared and named m2, m4, m6 and m8. These samples contain SLG and FLG, which were obtained by the micromechanical cleavage method from natural graphite and transferred to SiO_2 (280 nm)/Si substrates, followed by the deposition of Au-NPs. Before the deposition, the thickness of the graphene layer was checked by white light contrast microscopy [25].

The deposition of Au-NPs with different sizes on the graphene surface was carried out using the gas aggregation technique in a 4-gun commercial magnetron sputtering system (Further details can be found elsewhere [18]). The sets of samples were produced with different deposition times for two DC powers. At a power of 30 W, deposition times of 20 and 40 min were used for samples m2 and m4, whereas at a power of 60 W, 10 and 20 min of deposition were used for samples m6 and m8. After depositing the Au-NPs, the Raman spectra were acquired using a WITEC confocal (×100 objective) spectrometer with 600 lines/mm grating and 532 nm excitation energy, keeping the laser power at 1.0 mW to preclude or minimize the heating effect.

3. Results and discussion

Raman spectroscopy measurements were performed for SLG and FLG, in the presence and absence of gold nanoparticles. Fig. 1 shows optical image (a) and Raman maps (b–d) at four different regions (1–4) of the m4 sample after the deposition of Au-NPs. The Raman maps were performed taking into account different number of layers inside the square white of Fig. 1a. Fig. 1b was mapped with the integrated intensity of the G band (1580 cm^{-1}), where it is possible to see that the intensity of region 4 is higher than regions 3, 2 and particularly of region 1. Therefore, from this figure and a single spectrum of each region (before deposition of Au-NPs) we can infer that region 1 is a monolayer with a narrow FWHM (about 28 cm^{-1}), region 2 a bilayer (not studied here), region 3 encompasses about 3 layers and region 4 many layers. Fig. 1c and d shows the Raman Images mapped with the integrated intensities of the 2D bands at 2690 cm^{-1} (c) and 2671 cm^{-1} (d). Note that the intensity at 2690 cm^{-1} appears a bit higher in SLG (region 1) than in FLG (region 3), whereas for 2671 cm^{-1} the intensity is higher in region 1 than for the other regions, being a characteristic of monolayer graphene.

Simultaneously to the production of m2–m8 samples, additional samples with only the Au nanoparticles were produced on carbon
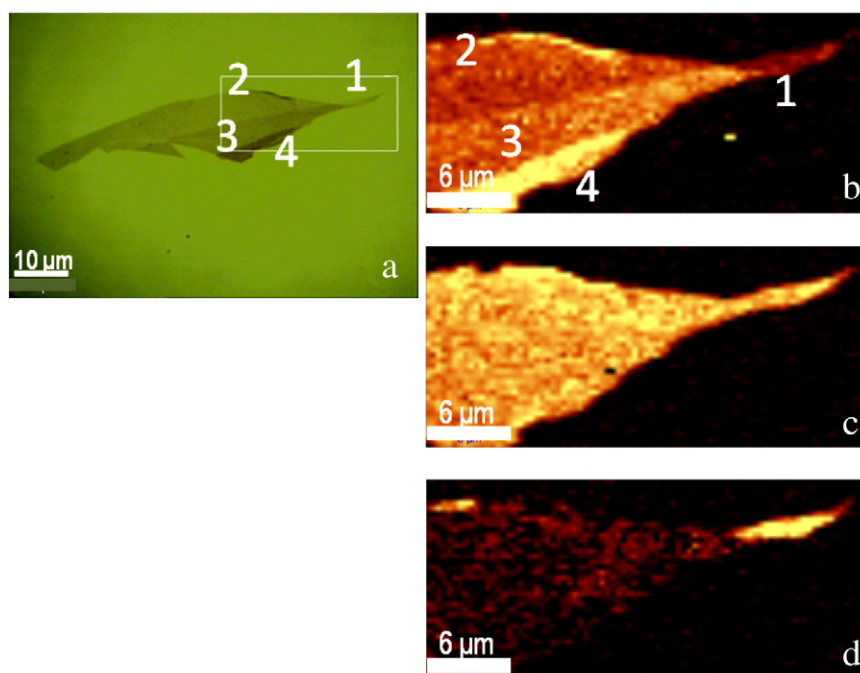
Fig. 1. Optical image of single (1), bi (2), few layers (3) and many layers (4) regions of graphene on SiO_2/Si substrate, for the sample m4, before deposition of Au-NPs (a). Raman images mapped with the integrated intensities of the G band (1580 cm^{-1}) (b) and 2D bands at 2690 cm^{-1} (c) and 2671 cm^{-1} (d) after deposition of Au-NPs.

coated Cu grids for transmission electron microscopy (TEM) analysis. It is clear from the TEM images (Fig. 2) that isolated Au-NPs are generated in a large extent using a power of 30 W, in contrast to 60 W. As a matter of fact, at 30 W/20 min (Fig. 2a) it is possible to see isolated nanoparticles (NP) of about 5 nm, in addition to a few aggregates, while, for the same power, after 40 min (Fig. 2b) the size of the NP increased, as well as, the formation of aggregates on the graphene surface. On the other hand, when the deposition power was kept at 60 W (Fig. 2c), the aggregates predominated.

The TEM results were corroborated by the UV–vis measurements (Fig. 2d) performed on the m2–m8 samples. Accordingly, for a power of 30 W, 20 min and 40 min the peaks maximum were found around 600 nm and ~720 nm. On the other hand, for a power of 60 W is not possible to observe a peak maximum, just a broad plateau spanning all range of wavelengths. This can be attributed to the presence of aggregates, as shown in Fig. 2c. It is well known that the UV–vis spectrum of single Au-NP consists of a narrow band with a peak maximum around 528 nm, which is named plasmon band [26]. As the size of the NPs and aggregates increases, this band suffers a broadening and shifts to a higher wavelength [21]. The broadening and red-shift of the absorption bands (Fig. 2d) of Au-NPs in SLG and FLG, with respect to the corresponding single Au-NPs at 528 nm, indicate the formation of Au-NPs aggregates on the graphene layers, which is consistent with the TEM results. This kind of behaviour has also been observed in colloidal solutions of Au-NPs of different sizes and shapes [27,28].

A comparison between the Raman measurements of SLG in the absence (black curve) and presence of Au-NPs can be seen in Fig. 3. At 30 W (m2, m4), the intensities of the G and 2D bands increase as the deposition time increases. This fact can be attributed to the increase of size and formation of aggregates, enhancing the extinction spectra in the visible (see Fig. 2).

At 60 W/10 min (m6), the Raman intensity also exhibits a small enhancement. The observed intensity is three times the Raman intensity observed at 30 W/20 min (m2) and almost equivalent to the
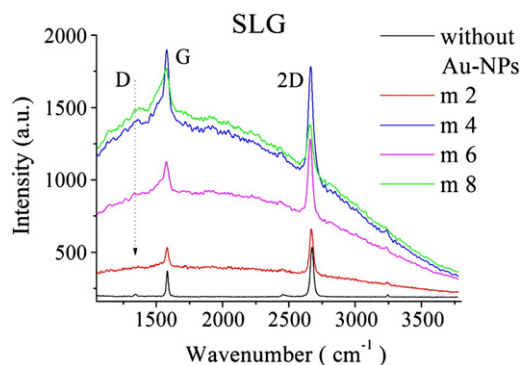
Fig. 3. Comparison of the Raman intensities of SLG graphene before (black curve, 1) and after deposition of Au-NPs at different power and deposition times. m2 (30 W/20 min., 2), m4 (30 W/40 min, 3), m6 (60 W/10 min., 4) and m8 (60 W/20 min, 5).

intensity recorded at 30 W/40 min (m4). The extinction profile shown in Fig. 2d exhibits an interesting feature around 550 nm, characteristic of large Au-NPs, in addition to the broad (plateau) plasmon coupling band above 700 nm. There is a good matching between the exciting radiation (532 nm) and the Au-NPs spectrum. It is interesting to note that at 60 W/20 min (m8), in spite of the larger deposition time, the heights of the G and 2D bands decreased, in contrast to the behaviour observed at 30 W. As one can see in Fig. 2d, as the nanoparticles size and aggregation increase at 60 W/20 min, the extinction profile shifts to longer wavelengths (>800 nm) leading to a mismatch with the available excitation wavelength of 532 nm. This aspect may be responsible for the observed decrease of intensity of the G and 2D bands (Fig. 3). On the other hand, with the increase of the Au-NPs size, a strong background appears on the Raman spectra due to the formation of large aggregates or films, as previously observed in photoluminescence (PL) studies on SLG [29].

In the same way, Fig. 4 shows a comparison of the Raman measurements before (black curve 1) and after the deposition of Au-NPs
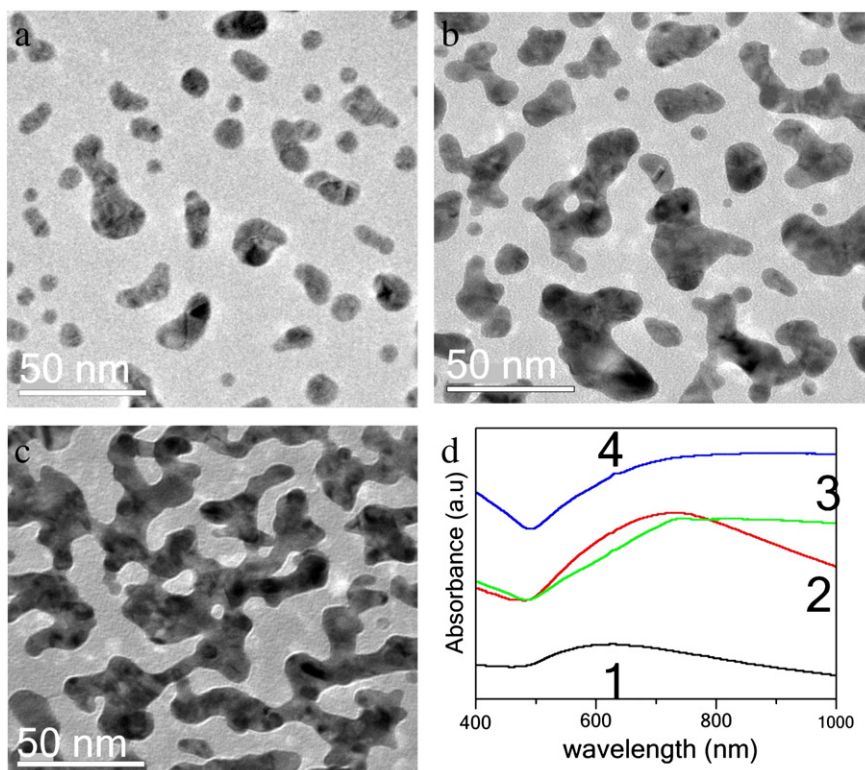
Fig. 2. TEM images of Au-NPs. a) 30 W/20 min, b) 30 W/40 min, c) 60 W/10 min and d) UV–vis spectra of the Au-NPs, shown in Fig. (a–c), 30 W/20 min (1, black), 30 W/40 min (2, red), 60 W/10 min (3, green) and 60 W/20 min (4, blue).
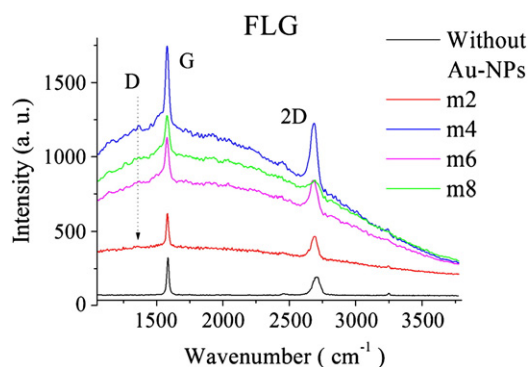
Fig. 4. Comparison of the Raman intensities of FLG before (black curve) and after deposition of Au-NPs (same colours as in Fig. 3, 1 = without Au-NPs, 2 = m2, 3 = m4, 4 = m6, 5 = m8).

Fig. 5. Integrated intensity ratio between the 2D band and G band (I_{2D}/I_G) of SLG (black dots) and FLG (empty dots) before (without Au-NPs) and after deposition of Au-NPs at the two DC powers and deposition times. As the time increases the ratio for SLG and FLG remains practically the same (30 W/40 min.).

onto FLG. Similarly, as in SLG, one can observe for FLG at a DC power of 30 W that the intensity of the G and 2D bands increases as the deposition time increases. On the other hand, for a power of 60 W the intensity of G and 2D bands decreases as the deposition time increases. In contrast to SLG, the intensity for 60 W/20 min is lower than the intensity for a power of 30 W/40 min.

There are two outstanding differences between Figs. 3 and 4. One is that the intensities of SLG, after deposition of Au-NPs, are higher than FLG, the second one is that the broadening of the G band in SLG is wider than the G band in FLG as the power and deposition time increase, particularly at 60 W/20 min.. On the other hand, for the same power and deposition time the broadening of the 2D band in FLG is wider than 2D band in SLG.

In order to evaluate the integrated intensities and FWHM of the G and 2D bands for SLG and FLG, the G band was deconvoluted using Lorentzian functions. In Table 1 one can find the G-peak frequency (ω_G (cm^{-1})), I_{2D}/I_G and FWHM for SLG and FLG for the different DC powers and depositions times. The results show that the G-peak frequency for SLG is more affected than for FLG, as the DC power increases.

In addition, the analyses from Figs. 3 and 4 (not shown here) showed that the Raman shift of the 2D band on SLG (Fig. 3) is more pronounced than the Raman shift of the G band, while for FLG (Fig. 4) the Raman shift it is nearly identical for the G band and 2D bands. According to the literature [23] there is an overall decrease of I_{2D}/I_G when the amount of charged impurities in graphene increases [30]. The blue shift in the G band has been used as indication of doping or charged impurities. On the other hand, the SLG samples without Au-NPs [31] seem to exhibit I_{2D}/I_G higher in the case of suspended graphene (SG) than for non-suspended graphene (NSG) samples. As a matter of fact, the I_{2D}/I_G intensity ratio provides more effective criterion for the selection of SLG sample exhibiting low impurity concentration levels ($<10^{12}$ cm^{-2}) for device-applications. Therefore, it is plausible that the shift of the G, 2D bands and the decrease of I_{2D}/I_G, in our samples are due to the presence of charge impurities, or to slightly doped SLG and FLG from the Au-NPs at increasing sizes and aggregation.

In order to rationalize the information on the effect of Au-NPs in SLG and FLG, the integrated intensity ratios between the 2D and G bands, I_{2D}/I_G, were plotted as a function of time in Fig. 5. From this Figure and Table 1, one can conclude that:

a) The I_{2D}/I_G ratio is always higher in SLG (filled black dots) than in FLG (empty black dots) for the two power and deposition times;
b) the I_{2D}/I_G ratio in SLG decreases from 2.9 (without Au-NPs) to 1.07 (with Au-NPs) for a power of 60 W/20 min, in agreement with a previous report [26] of a ratio of 2.4 for SLG before and 1.4 after the deposition of Au-NPs. For FLG, it is almost constant in all the range of power and deposition times. The sizes and Au-NPs aggregates have a negligible effect on I_{2D}/I_G for FLG.
c) The FWHM of both G (Fig. 3) and 2D bands (Fig. 4) increases for SLG and FLG as the DC power and deposition times increase. According to the literature [25], a charge-transfer between Au-NPs and graphene can be responsible for the increase of the FWHM(G).

Another interesting feature in our results is the relatively low intensity of the D band (traced arrows in Figs. 3 and 4) due to the increase of disorder as the size of the Au-NPs and aggregates increases.

In Fig. 6, FWHM(G) was plotted as a function of ω_G (cm^{-1}) for SLG (filled dots) and FLG (empty dots). One can see that as the ω_G (cm^{-1}) decreases, FWHM(G) increases. This observation has also been reported in FLG samples after interaction with 1 M (g/mol) solutions of various monosubstituted benzenes (aniline) with electron-donating groups [32]. They argued that such marked effects (decrease of the G band) are due to molecular charge-transfer even with multi-layered graphene encompassing 3–4 layers. In addition to this, it has been observed shifts of the G band of single-walled carbon nanotubes

Table 1
Set of G-frequency peaks (ω_G (cm^{-1})), I_{2D}/I_G and FWHM for SLG and FLG, for the different DC power and deposition times.

Power(W)/time (min)	ω_G (cm^{-1})		I_{2D}/I_G		FWHM(G) (cm^{-1})	
	SLG	FLG	SLG	FLG	SLG	FLG
Without Au-NPs	1583	1584	2.9	1.4	17	19
30/20	1577	1578	2.4	1.8	27	20
30/40	1573	1576	1.45	1.44	35	28
60/10	1570	1575	1.84	1.34	38	29
60/20	1569	1574	1.0	0.9	52	32
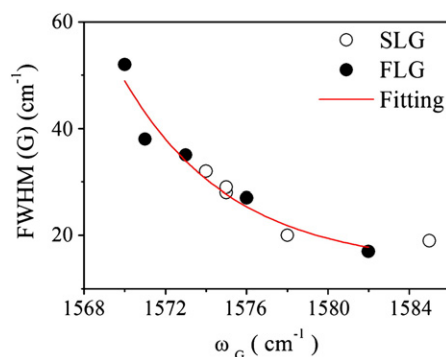
Fig. 6. FWHM(G) as a function of the G peak frequency (cm^{-1}) for SLG (black dots) and FLG (empty dots). Red line is a fitting of the experimental values.

(SWNTs) on interaction with varying concentrations of tetrathiaful-valene (TTF), as well as, an increase of a small shoulder at low frequency of the main peak G band [33]. On the other hand, there is a broadening, at low frequency, of the G band lineshape of metallic SWNTs, which is related to the presence of free electrons in nanotubes with metallic character [34]. In spite of the fact that SWNTs and SLG or FLG are different systems, they are carbon related materials and are in accordance with our results. Furthermore, carbon nanotubes doped with boron and nitrogen produced shifts in the opposite directions just as nitrobenzene and aniline [33]. While boron doping (p-type) increases the G band frequency, nitrogen doping (n-type) decreases the G band frequency, similar to our results. Finally, the fitting between ω_G and FWHM(G) shown in Fig. 6 plots is in agreement with the theoretical correlation [30]. One can also see a similar behaviour for FWHM(G) in both SLG and FLG. The charge impurities and doping in graphene must be higher in our samples than in samples without Au-NPs. Therefore, taking into account these results, we surmise that Au-NPs of different sizes and aggregates can cause n-type doping in SLG and FLG samples.

4. Conclusions

The graphene Raman intensity depends on the sizes and aggregation of Au-NPs. Probably, the electronic interactions of the Au-NPs with the graphene sheet are the main responsible for the changes in the Raman spectra. In addition, an unintentional doping of the SLG and FLG surfaces introduced by the Au-NPs at increasing sizes and aggregates was detected by the decrease of the integrated intensity ratio, I_{2D}/I_G, with the increase of the power and deposition times. This fact was corroborated by the shift of the G and 2D band to lower frequencies, and increase of the FWHM(G) with the decrease of ω_G (cm^{-1}) in SLG and FLG.

References

[1] K.S. Novoselov, A.K. Geim, S.V. Morozov, D. Jiang, Y. Zhang, S.V. Dubonos, I.V. Grigorieva, A.A. Firsov, Science 306 (2004) 666.
[2] K.S. Novoselov, A.K. Geim, S.V. Morozov, D. Jiang, M.I. Katsnelson, I.V. Grigorieva, S.V. Dubonos, Nature 438 (2005) 197.
[3] K.S. Novoselov, E. McCann, S.V. Morozov, V.I. Fal'ko, M.I. Katsnelson, U. Zeitler, D. Jiang, F. Schedin, A.K. Geim, Nat. Phys. 2 (177) (2006).
[4] A.K. Geim, K.S. Novoselov, Nat. Mater. 6 (2007) 183.
[5] K.S. Kim, Y. Zhao, H. Jang, S.Y. Lee, J.M. Kim, J.H. Ahn-Kim, J.Y.P. Choi, B.H. Hong, Nature 457 (2009) 706.
[6] A.V. Eletskii, I.M. Iskandarova, A.A. Knizhnik, D.N. Krasikov, Physics-Uspekhi 54 (3) (2011) 227.
[7] A.C. Ferrari, J.C. Meyer, V. Scardaci, C. Casiraghi, M. Lazzeri, F. Mauri, S. Piscanec, D. Jiang, K.S. Novoselov, S. Roth, A.K. Geim, Phys. Rev. Lett. 97 (2006) 187401.
[8] A. Das, B. Chakraborty, K. Sood, Bull. Mater. Sci. 31 (3) (2008) 579.
[9] I. Calizo, S. Ghosha, W. Baob, F. Miaob, C. Ning Lau, A.A. Balandin, Solid State Commun. 149 (2009) 1132.
[10] Y.Y. Wang, Z. Hua Ni, T. Yu, Z.X. Shen, H.M. Wang, Y.H. Wu, W. Chen, T.S. Wee, J. Phys. Chem. C 112 (2008) 10637.
[11] R. Yang, Q.S. Huang, X.L. Chen, G.Y. Zhang, H.J. Gao, J. Appl. Phys. 107 (2010) 034305.
[12] I. Calizo, I. Bejenari, M. Rahman, G. Liu, A.A. Balandin, Appl. Phys. 106 (2009) 043509.
[13] A. Das, S. Pisana, B. Chakravorty, S. Piscanec, S.K. Saha, U.V. Waghmare, K.S. Novoselov, H.R. Krishnamurthy, R.A.K. Geim, A.C. Ferrari, A.K. Sood, Nat. Nanotechnol. 3 (2008) 210.
[14] J. Yan, Y. Zhang, P. Kim, A. Pinczuk, Phys. Rev. Lett. 98 (2007) 166802.
[15] M. Lazzeri, S. Piscanec, F. Mauri, A.C. Ferrari, J. Robertson, Phys. Rev. B 73 (2006) 155426.
[16] C. Casiraghi, S. Pisana, K.S. Novoselov, A.K. Geim, A.C. Ferrari, Appl. Phys. Lett. 91 (2007) 233108/1-233108/3.
[17] X. Dong, D. Fu, W. Fang, Y. Shi, P. Chen, L. -Jong, Nano e Micro Small, 5 (12), Wiley Interscience, 2009, p. 1422.
[18] Z.H. Ni, H.M. Wang, J. Kasim, H.M. Fan, T. Yu, Y.H. Wu, Y.P. Feng, Z.X. Shen, Nano Lett. 7 (2007) 2758.
[19] H.J. Shin, S.M. Kim, S.M. Yoon, A. Benayad, K.K. Kim, S.J. Kim, H. Ki Park, J.Y. Choi, Y.H. Lee, J. Am. Chem. Soc. 130 (2008) 2062.
[20] R. Voggu, C.S. Rout, A.D. Franklin, T.S. Fisher, C.N.R. Rao, J. Phys. Chem. C 112 (2008) 13053.
[21] C. Casiraghi, A. Hartschuh, E. Lidorikis, H. Qian, H. Harutyunyan, T. Gokus, K.S. Novoselov, A.C. Ferrari, Nano Lett. 7 (2007) 2711.
[22] R. Muszynski, B. Seger, P.V. Kamat, J. Phys. Chem. Lett. 112 (2008) 5263.
[23] Y.-H. Lu, M. Zhou, C. Zhang, Y.-P. Feng, J. Phys. Chem. Lett. 113 (2009) 20156.
[24] G.T. Landi, S.A. Romero, A.D. Santos, Rev. Sci. Instrum. 81 (2010) 033908.
[25] J. Huang, L. Zhang, B. Chen, N. Ji, F. Chen, Y. Zhang, Z. Zhang, Nanoscale 2 (2010) 2733–2738.
[26] J. Lee, S. Shim, B. Kim, H.S. Shin, Chem. Eur. J. 17 (2011) 2381–2387.
[27] J. Hu, Z. Wang, J. Li, Sensors 7 (2007) 3299–3311.
[28] Y. Wang, Z. Ni, H. Hu, Y. Hao, C. Pei-Wong, T. Yu, J.T.L. Thong, Z. Xiang- Shen, Appl. Phys. Lett. 97 (2010) 163111.
[29] Y. Wang, Z. Ni, H. Hu, Y. Hao, C. Pei-Wong, T. Yu, J.T.L. Thong, Z. Xiang- Shen, Applied Phys. Lett. 97 (2010) 163111.
[30] C. Casiraghi, S. Pisana, K.S. Novoselov, A.K. Geim, A.C. Ferrari, Appl. Phys. Lett. 91 (2007) 233108.
[31] Z. Hua-Ni, T. Yu, Z. Qiang-Luo, Y. Ying-Wang, L. Liu, C. Pei-Wong, J. Miao, W. Huang, Z. Xiang-Shen, ACS Nano 3 (2009) 569.
[32] B. Das, R. Voggu, C. Sekhar Rout, C.N.R. Rao, Chem. Commun. (2008) 5155–5157.
[33] R. Voggu, C. Seakhar Rout, A.D. Franklin, T.S. Fisher, C.N.R. Rao, J. Chem. Phys. C 112 (130) (2008) 53.
[34] A. Jorio, M.A. Pimenta, A.G. Souza Filho, R. Saito, G. Dresselhaus, M.S. Dresselhaus, New J. Phys. 5 (2003) 139.1–139.17.